ISSN 0006-2979, Biochemistry (Moscow), 2011, Vol. 76, No. 11, pp. 1253-1261. © Pleiades Publishing, Ltd., 2011.
Published in Russian in Biokhimiya, 2011, Vol. 76, No. 11, pp. 1556-1565.

Characteristics of Protection by MgADP and MgATP of $\alpha_3\beta_3\gamma$ Subcomplex of Thermophilic *Bacillus* PS3 βY341W-mutant F_1-ATPase from Inhibition by 7-Chloro-4-nitrobenz-2-oxa-1,3-diazole Support a Bi-site Mechanism of Catalysis

Y. M. Milgrom

Department of Biochemistry and Molecular Biology, State University of New York, Upstate Medical University, Syracuse, New York 13210, USA; fax: +1-315-464-8750; E-mail: milgromy@upstate.edu

Received January 21, 2011
Revision received April 5, 2011

Abstract—MgADP and MgATP binding to catalytic sites of βY341W-$\alpha_3\beta_3\gamma$ subcomplex of F_1-ATPase from thermophilic *Bacillus* PS3 has been assessed using their effect on the enzyme inhibition by 7-chloro-4-nitrobenz-2-oxa-1,3-diazole (NBD-Cl). It was assumed that NBD-Cl can inhibit only when catalytic sites are empty, and inhibition is prevented if a catalytic site is occupied with a nucleotide. In the absence of an activator, MgADP and MgATP protect βY341W-$\alpha_3\beta_3\gamma$ subcomplex from inhibition by NBD-Cl by binding to two catalytic sites with an affinity of 37 μM and 12 mM, and 46 μM and 15 mM, respectively. In the presence of an activator lauryldimethylamine-N-oxide (LDAO), MgADP protects βY341W-$\alpha_3\beta_3\gamma$ subcomplex from inhibition by NBD-Cl by binding to a catalytic site with a K_d of 12 mM. Nucleotide binding to a catalytic site with affinity in the millimolar range has not been previously revealed in the fluorescence quenching experiments with βY341W-$\alpha_3\beta_3\gamma$ subcomplex. In the presence of activators LDAO or selenite, MgATP protects βY341W-$\alpha_3\beta_3\gamma$ subcomplex from inhibition by NBD-Cl only partially, and the enzyme remains sensitive to inhibition by NBD-Cl even at MgATP concentrations that are saturating for ATPase activity. The results support a bi-site mechanism of catalysis by F_1-ATPases.

DOI: 10.1134/S0006297911110071

Key words: ATP synthase, catalytic cooperativity, bi-site catalysis, multi-site catalysis, nucleotide binding

In the energy-transforming membranes of mitochondria, chloroplasts, and bacteria, reversible ATP synthesis/hydrolysis coupled to transmembrane transport of H^+ is catalyzed by a multisubunit complex – F_oF_1-ATP synthase. This complex can be separated into a soluble catalytic component F_1-ATPase that consists of five types of subunits in a stoichiometry of $\alpha_3\beta_3\gamma\delta\varepsilon$, and a membrane-embedded component F_o that in bacteria is formed by *a*, *b*, and a ring of *c* subunits in a stoichiometry of ab_2c_{10}. F_1 has three catalytic and three noncatalytic nucleotide-binding sites formed by the major β and α subunits [1]. In addition, isolated ε subunit [2] and γε-subcomplex [3] of TF_1 have been reported to bind an ATP molecule. In the high-resolution crystal structure of MF_1, α and β subunits are arranged alternately around the γ subunit with the catalytic and noncatalytic sites located alternately at the six α/β interfaces [4]. It is generally accepted that F_oF_1-ATP synthase operates according to the rotary binding change mechanism proposed by Boyer and colleagues [5-7]. It is thought that binding changes at the F_1 catalytic sites are coupled to proton transport through F_o via rotation of a complex of subunits (rotor, $\gamma\varepsilon c_{10}$ in bacteria) within a stator that in bacteria is formed by $\alpha_3\beta_3\delta ab_2$ [8, 9]. ATP-dependent rotation of a rotor component (γ subunit) relative to a stator ($\alpha_3\beta_3$) was first

Abbreviations: BSA, bovine serum albumin; F_1, the solubilized portion of F_oF_1-ATP synthase; LDAO, lauryldimethylamine-N-oxide; MF_1, EcF_1, and TF_1, F_1-ATPases from mitochondria, *Escherichia coli*, and thermophilic *Bacillus* PS3, respectively; NBD-Cl, 7-chloro-4-nitrobenz-2-oxa-1,3-diazole; PEP, phosphoenolpyruvate.

directly demonstrated with $\alpha_3\beta_3\gamma$ subcomplex of TF_1 [10], and, subsequently, relative rotation involving other components of rotor and stator has been also directly observed [11-13]. In the presence of ADP and P_i, forced rotation of the γ subunit in the direction opposite to that observed during ATP hydrolysis has been shown to result in a net ATP synthesis by the $\alpha_3\beta_3\gamma$ subcomplex [14].

According to the binding change mechanism, the enzyme turnover is slow and limited by the product dissociation when only one of F_1 catalytic sites is occupied, but the turnover is accelerated when substrate binds at the additional catalytic site(s) that sequentially participate in catalysis [7]. This strong positive catalytic cooperativity was first quantified for ATP hydrolysis by MF_1 to result in a 10^6-fold acceleration of the turnover rate [15]. Slow F_1 turnover with only one catalytic site occupied has been named uni-site catalysis [16], and the cooperative mode of F_1 turnover (multi-site catalysis) has been referred to as bi-site or tri-site catalysis depending on the presumed extent of catalytic site occupancy [15]. It has been initially suggested that substrate binding at a second catalytic site provides the major kinetic enhancement seen in multi-site catalysis [15, 17]. However, the matter of whether a bi-site or tri-site model of catalysis is responsible for positive catalytic cooperativity of F_1 has remained controversial. The results obtained in studies of transition to multi-site catalysis during ATP synthesis by chloroplasts [18] and ATP hydrolysis by MF_1 [19], in studies of competition between ATP and TNP-ATP for binding to MF_1 [20], and in studies of catalytic site occupancy during multi-site ATP hydrolysis by MF_1 [21] and EcF_1 [22] using a centrifugal filtration method, all strongly support a bi-site model of multi-site catalysis. On the other hand, main support for a tri-site model of catalysis has been provided by the fluorescence studies first carried out with βY331W-mutant EcF_1 [23] and subsequently with the homologous βY341W-mutant $\alpha_3\beta_3\gamma$ subcomplex of TF_1 [24, 25] and βY345W-mutant MF_1 from the yeast *Saccharomyces cerevisiae* [26]. In these studies, the extent of catalytic-site occupancy during ATP hydrolysis was ascertained using nucleotide-induced quenching of fluorescence of the engineered tryptophan residues with the assumption that nucleotide binding at all three catalytic sites could be detected. The results were interpreted as supporting a tri-site model regardless of whether the contribution of nucleotide binding at each of the three catalytic sites to the overall fluorescence quenching was considered to be the same [23, 24, 26] or not [25].

The validity of the interpretation of the fluorescence quenching data in favor of a tri-site model has been recently challenged by Bulygin and Milgrom [27] who have shown that nucleotide-concentration dependence of βY331W-EcF_1 fluorescence quenching by ADP, ATP, and MgADP is biphasic with each phase contributing about equally to the total nucleotide-induced quenching. These results as well as similar results obtained in the other studies when fluorescence of βY331W-EcF_1 was quenched by MgADP [23, 28-30] and MgAMPPNP [23, 31] and fluorescence of βY341W-mutant $\alpha_3\beta_3\gamma$ subcomplex of TF_1 was quenched by MgADP and MgATP [32, 33] make it highly unlikely that the extent of fluorescence quenching correctly reports the extent of occupancy of three catalytic sites in the enzyme. Moreover, analysis of the data obtained by Senior and colleagues with βY331W-EcF_1 that contained a series of additional second mutations [34-38] on MgADP-induced fluorescence quenching and MgADP-induced protection from inactivation by 7-chloro-4-nitrobenz-2-oxa-1,3-diazole (NBD-Cl) – a well known inhibitor of F_1-ATPases [39] that specifically reacts with the homologous tyrosine residues in β subunits (βY311 in MF_1 [40, 41] and βY307 in TF_1 [42, 43]) – has led to a conclusion [27] that nucleotide binding at the third (lowest affinity) catalytic site contributes little if at all to the overall nucleotide-induced fluorescence quenching. This conclusion is supported by the recent results obtained with EcF_1 containing only the βY331W-mutation [44]. The results show that MgADP-induced protection of βY331W-EcF_1 from inhibition by NBD-Cl is due to the nucleotide binding to a catalytic site with a K_d of about 10 mM [44]. Such a binding escaped detection when MgADP binding to the catalytic sites of βY331W-EcF_1 was probed using the fluorescence-quenching approach [23, 27, 28, 30, 45, 46].

In the present paper, it was examined whether nucleotide binding to the lowest affinity catalytic site of βY341W-$\alpha_3\beta_3\gamma$ subcomplex of TF_1 could have escaped detection in the fluorescence-quenching studies as it did in the studies with βY331W-EcF_1. To this aim, it was investigated how MgADP and MgATP protected βY341W-$\alpha_3\beta_3\gamma$ subcomplex from inhibition by NBD-Cl. The data show that these nucleotides bind to the lowest affinity catalytic site of βY341W-$\alpha_3\beta_3\gamma$ subcomplex with a K_d of 12 mM and ≥15 mM, respectively. Such a binding is not reflected in the nucleotide-induced fluorescence quenching reported for βY341W-$\alpha_3\beta_3\gamma$ subcomplex [24, 25, 32, 33, 47, 48]. The results show that nucleotide binding to the third catalytic site of βY341W-$\alpha_3\beta_3\gamma$ subcomplex of TF_1, as in the case of βY331W-EcF_1, occurs without a significant contribution to the total nucleotide-induced fluorescence quenching and support a bi-site mechanism of ATP hydrolysis by F_1.

MATERIALS AND METHODS

Materials. ADP, ATP, NADH, Tris, triethanolamine, bovine serum albumin (BSA), pyruvate kinase, and lyophilized lactate dehydrogenase were from Sigma (USA). Mops and potassium phosphoenolpyruvate (PEP) were from Fluka (USA); H_2SeO_3 was from Aldrich (USA); dimethyl sulfoxide was from Baker (USA); and lauryldimethylamine-N-oxide (LDAO) was from Calbiochem (USA). NBD-Cl was from Pierce (USA). Stock solutions

of NBD-Cl (50 mM) were prepared in dry dimethyl sulfoxide and stored at −20°C protected from light. $KHSeO_3$ was prepared by titrating the H_2SeO_3 solution with KOH to pH 8.0. The pH of the stock solutions of ADP, ATP and PEP was adjusted to 8.0 with triethanolamine.

An αW463Y/βY341W-$\alpha_3\beta_3\gamma$ subcomplex of TF_1 [49] containing additionally a His_{10}-tag at the N-terminus of β subunits (subsequently referred to in this paper as βY341W-$\alpha_3\beta_3\gamma$ subcomplex) and purified as described [50] with an additional anion-exchange chromatography step using DEAE-Toyopearl 650S was generously provided by Dr. Masasuke Yoshida and Dr. Toshiharu Suzuki. For the experiments, an ammonium sulfate suspension of the subcomplex was centrifuged, and the precipitate was dissolved in a buffer containing 20 mM Mops/triethanolamine, pH 8.0, and 0.2 mM EDTA (MTE buffer). The βY341W-$\alpha_3\beta_3\gamma$ subcomplex solution was then desalted by column centrifugation method [51] using columns equilibrated with MTE buffer, and the subcomplex was stored in small aliquots at −80°C until use. The A_{280}/A_{260} ratio of the preparations was 2.0 and corresponded to an adenine nucleotide content of less than 0.1 mol/mol of subcomplex [52, 53]. Concentration of the subcomplex was calculated using absorbance at 280 nm and an extinction coefficient of $1.54 \cdot 10^5$ $M^{-1} \cdot cm^{-1}$ [54].

Inhibition of βY341W-$\alpha_3\beta_3\gamma$ subcomplex by NBD-Cl. To investigate the effect of MgADP on inhibition of βY341W-$\alpha_3\beta_3\gamma$ subcomplex by NBD-Cl, 20 nM subcomplex was preincubated at room temperature (20-22°C) for 2 min in MTE buffer containing additionally 2.2 mM $Mg(CH_3COO)_2$, 0.2 mg/ml pyruvate kinase, and 0.3 mg/ml BSA in the absence and presence of MgADP (prepared using equimolar amounts of ADP and $Mg(CH_3COO)_2$) and 0.06% LDAO. Then NBD-Cl was added from 50-mM stock solution to obtain the final concentration of 0.15 mM unless indicated otherwise, and ATPase activity was measured as described below using 40-μl aliquots of the reaction mixture after additional incubation for 0.5-12 min. When MgADP concentration exceeded 1 mM, the subcomplex concentration was increased to 80 nM and the volume of reaction mixture aliquots used to assay the ATPase activity was decreased to 10 μl. Control experiments showed that incubation of βY341W-$\alpha_3\beta_3\gamma$ subcomplex as described above in the absence and presence of MgADP and/or LDAO but without NBD-Cl did not affect the ATPase activity.

To investigate the effect of MgATP on inhibition of βY341W-$\alpha_3\beta_3\gamma$ subcomplex by NBD-Cl, 10 nM subcomplex was preincubated at room temperature for 2 min in MTE buffer containing additionally 10 mM CH_3COOK, 2.2 mM $Mg(CH_3COO)_2$, 1 mM PEP, 0.2 mg/ml pyruvate kinase, and 0.3 mg/ml BSA in the absence and presence of MgATP (prepared using equimolar amounts of ATP and $Mg(CH_3COO)_2$; a constant 2-mM excess of Mg^{2+} ensured that the nucleotide was completely complexed with Mg^{2+}). Then NBD-Cl was added from 50-mM stock solution to obtain the final concentration of 0.15 mM, and ATPase activity was measured as described below using 40-μl aliquots of the reaction mixture after additional incubation for 0.5-12 min. Control experiments showed that incubation of βY341W-$\alpha_3\beta_3\gamma$ subcomplex as described above in the absence and presence of MgATP did not affect the ATPase activity. When the effect of MgATP was probed in the presence of 0.06% LDAO or 10 mM $KHSeO_3$, the βY341W-$\alpha_3\beta_3\gamma$ subcomplex concentration was decreased to 5 nM, the PEP concentration was increased to 1.5 mM, and the preincubation time was increased to 15 and 8 min, respectively. Less than 70% of the added PEP was consumed in the course of experiments with MgATP even in the absence of NBD-Cl.

The apparent pseudo first-order rate constants of βY341W-$\alpha_3\beta_3\gamma$ subcomplex inhibition by NBD-Cl (k) were obtained by fitting the data to equation:

$$A_t = A_1 + A_2 e^{-kt}, \quad (1)$$

where A_t is ATPase activity of βY341W-$\alpha_3\beta_3\gamma$ subcomplex after incubation with NBD-Cl for a time t.

ATPase activity assay. ATPase activity of βY341W-$\alpha_3\beta_3\gamma$ subcomplex was measured spectrophotometrically [55] at 340 nm at 30°C. The assay medium (final volume 1 ml) contained MTE buffer, 4.2 mM $Mg(CH_3COO)_2$, 10 mM CH_3COOK, 1 mM PEP, 2 mM ATP, 0.3 mM NADH, 0.06% LDAO, 0.1 mg/ml pyruvate kinase, and 0.1 mg/ml lactate dehydrogenase. As reported earlier for $\alpha_3\beta_3\gamma$ subcomplexes lacking [56] and containing βY341W mutation [32, 57], the kinetics of ATP hydrolysis by βY341W-$\alpha_3\beta_3\gamma$ subcomplex exhibits a lag phase due to presence of LDAO. Under the assay conditions described above, this lag phase lasted about 2 min. For this reason, the ATPase activity was calculated using the slope of the linear part of the absorbance recording observed during the last 4 min of the 7-min assay. Molar activity of βY341W-$\alpha_3\beta_3\gamma$ subcomplex was 400 sec^{-1}. ATPase activity of the samples containing NBD-Cl was calculated after correcting for a small rate of absorbance decrease due to presence of NBD-Cl determined using samples lacking βY341W-$\alpha_3\beta_3\gamma$ subcomplex.

MgATP-concentration dependence of βY341W-$\alpha_3\beta_3\gamma$ subcomplex steady-state activity at room temperature was measured in MTE buffer containing additionally 2.2 mM $Mg(CH_3COO)_2$, 10 mM CH_3COOK, 1 mM PEP, 0.3 mM NADH, MgATP (prepared using equimolar amounts of ATP and $Mg(CH_3COO)_2$), 0.1 mg/ml pyruvate kinase, and 0.1 mg/ml lactate dehydrogenase in the absence and presence of 0.06% LDAO or 10 mM $KHSeO_3$.

RESULTS AND DISCUSSION

Figure 1a shows time-course of βY341W-$\alpha_3\beta_3\gamma$ subcomplex inhibition by 0.05 mM (curve *1*), 0.1 mM (curve

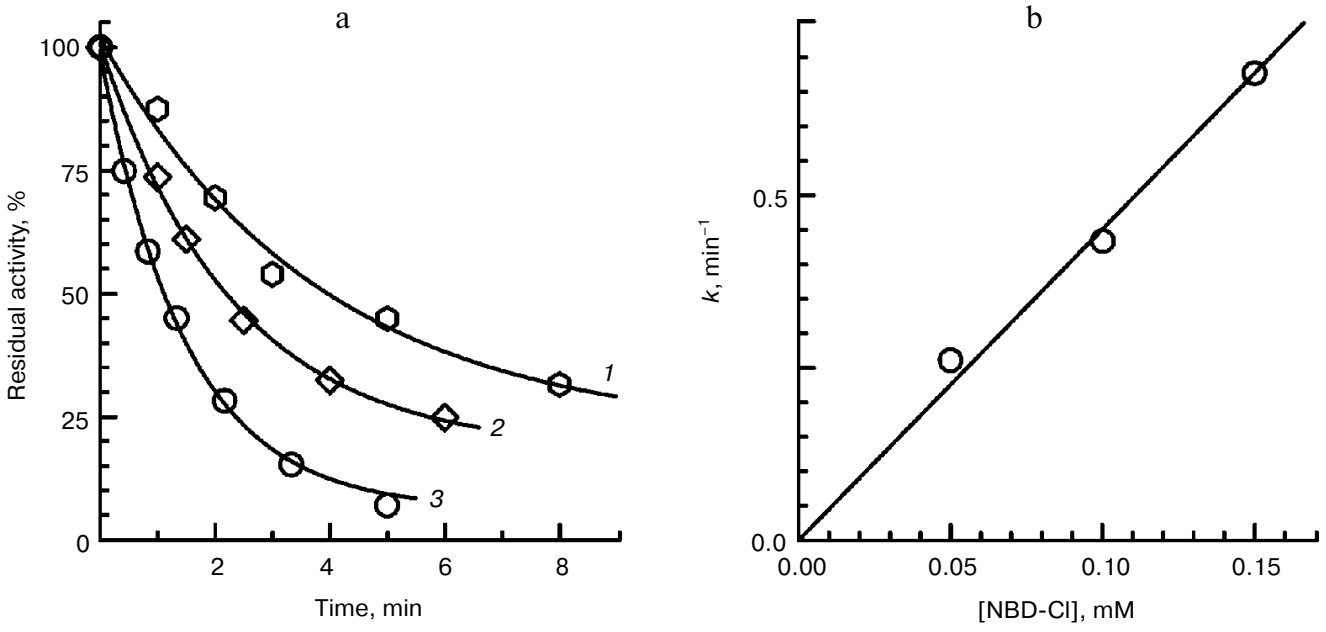

Fig. 1. Inhibition of βY341W-$\alpha_3\beta_3\gamma$ subcomplex by NBD-Cl. a) Time course of βY341W-$\alpha_3\beta_3\gamma$ subcomplex inhibition by 0.05 (*1*), 0.1 (*2*), and 0.15 mM (*3*) NBD-Cl. b) Effect of NBD-Cl concentration on the pseudo-first order rate constant k of βY341W-$\alpha_3\beta_3\gamma$ subcomplex inhibition. Rate constants k were obtained from the data shown in panel (a) as described in "Materials and Methods". Slope of the line obtained using the linear regression analysis is equal to $(4.4 \pm 0.3)\cdot10^3$ $M^{-1}\cdot min^{-1}$.

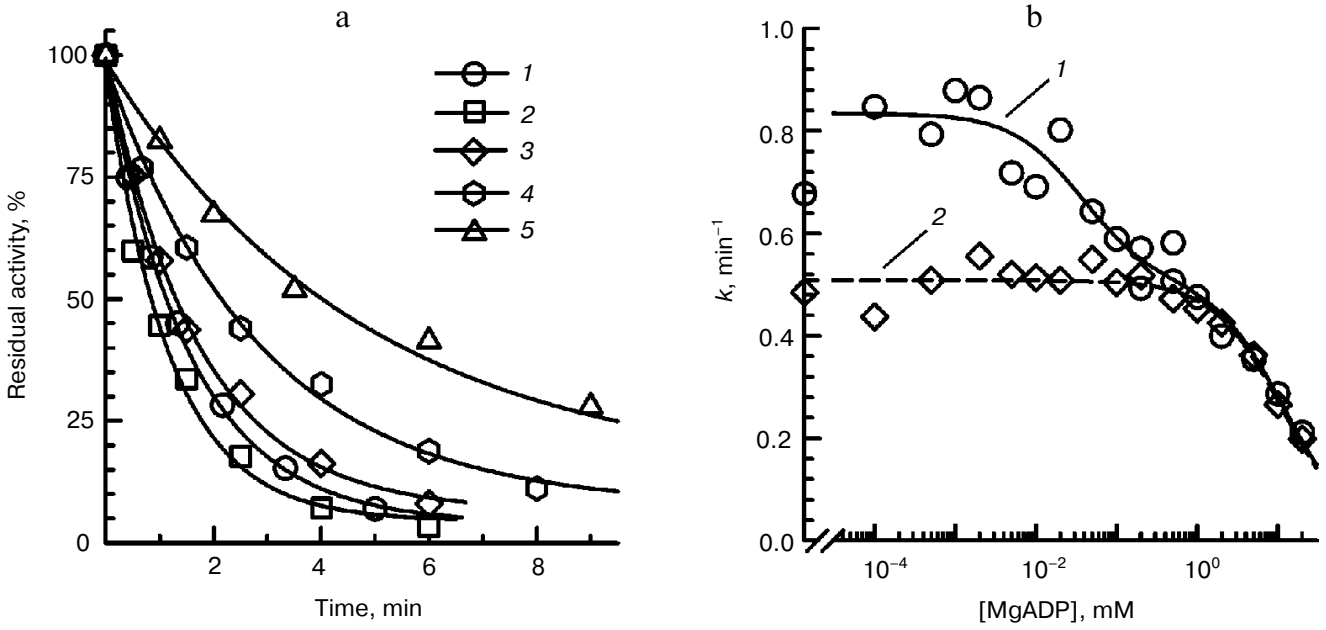

Fig. 2. Effect of MgADP on inhibition of βY341W-$\alpha_3\beta_3\gamma$ subcomplex by 0.15 mM NBD-Cl. a) Time course of βY341W-$\alpha_3\beta_3\gamma$ subcomplex inhibition by 0.15 mM NBD-Cl in the absence (*1*) and presence of 0.1 μM (*2*), 0.5 mM (*3*), 5 mM (*4*), and 20 mM (*5*) MgADP. b) Effect of MgADP concentration on the rate constant k of βY341W-$\alpha_3\beta_3\gamma$ subcomplex inhibition by 0.15 mM NBD-Cl in the absence (*1*) and presence of 0.06% LDAO (*2*). Rate constants k were obtained as described in "Materials and Methods". Solid line represents the best fit of the data obtained in the absence of LDAO to Eq. (2) with the values of k_2, k_3, K_{d2}, and K_{d3} equal to 0.33 ± 0.04 min^{-1}, 0.51 ± 0.04 min^{-1}, 37 ± 20 μM, and 12 ± 4 mM, respectively. Dashed line represents the best fit of the data obtained in the presence of LDAO to Eq. (3) with the values of k_0 and K_d equal to 0.508 ± 0.008 min^{-1} and 12 ± 2 mM, respectively.

2), and 0.15 mM (curve *3*) NBD-Cl. The values of the apparent first-order rate constants *k* obtained by fitting the data shown in Fig. 1a to Eq. (1) are plotted in Fig. 1b versus the corresponding NBD-Cl concentrations. It is seen in Fig. 1b that, in the range of NBD-Cl concentrations up to 0.15 mM, there is a linear dependence between *k* values and NBD-Cl concentrations. This fact means that in the studied range of NBD-Cl concentrations the rate of βY341W-$\alpha_3\beta_3\gamma$ subcomplex inactivation by NBD-Cl is limited by the rate of the inhibitor binding to the subcomplex.

Figure 2a shows time-course of βY341W-$\alpha_3\beta_3\gamma$ subcomplex inhibition by 0.15 mM NBD-Cl in the absence (curve *1*) and presence of 0.1 μM (curve *2*), 0.5 mM (curve *3*), 5 mM (curve *4*), and 20 mM (curve *5*) MgADP. Curve *1* in Fig. 2b shows MgADP concentration dependence of the apparent first-order rate constants *k* of the subcomplex inactivation by 0.15 mM NBD-Cl. It is seen that MgADP at the lowest concentration tested (0.1 μM) accelerates inhibition of βY341W-$\alpha_3\beta_3\gamma$ subcomplex by NBD-Cl. Similar effect of low concentrations of MgADP on inhibition by NBD-Cl has been observed with the wild-type EcF_1 but not with βY331W-EcF_1 [44]. With βY341W-$\alpha_3\beta_3\gamma$ subcomplex, increasing MgADP concentration above 2 μM results in a two-phase decrease of the inhibition rate. Such a MgADP-concentration dependence of *k* indicates that MgADP modulation of the βY341W-$\alpha_3\beta_3\gamma$ subcomplex inhibition by NBD-Cl is due to nucleotide binding at more than one catalytic site. A satisfactory fit (solid line, Fig. 2b) was obtained when the data obtained in the presence of MgADP were fitted to equation:

$$k = k_2/(1 + S/K_{d2}) + k_3/(1 + S/K_{d3}), \qquad (2)$$

where *S* is the concentration of MgADP. Equation (2) is based on a model that assumes that MgADP at saturating concentration completely protects the enzyme from inhibition by NBD-Cl, and that independent MgADP binding at two catalytic sites (designated as sites 2 and 3) with K_{d2} and K_{d3}, respectively, results in a decrease of the rate constant of βY341W-$\alpha_3\beta_3\gamma$ subcomplex inhibition (k_2 and k_3, respectively) by NBD-Cl. The best fit values of k_2 and k_3 are equal to 0.33 ± 0.04 and 0.51 ± 0.04 min^{-1}, respectively, and the best fit values of K_{d2} and K_{d3} are equal to 37 ± 20 μM and 12 ± 4 mM, respectively. Practically indistinguishable results of the best fit were obtained when MgADP binding to the catalytic sites 2 and 3 was assumed to be sequential. When MgADP-induced fluorescence quenching was used as a signal, the K_d values of 14-34 μM were obtained for the lowest affinity catalytic site of βY341W-$\alpha_3\beta_3\gamma$ subcomplex [24, 32, 33]. These values are significantly lower than the K_{d3} value for MgADP of 12 mM obtained from the data of Fig. 2b (curve *1*), but are close to the K_{d2} value of 37 μM.

Curve *1* in Fig. 3 shows the effect of MgATP on inhibition of βY341W-$\alpha_3\beta_3\gamma$ subcomplex by NBD-Cl. These

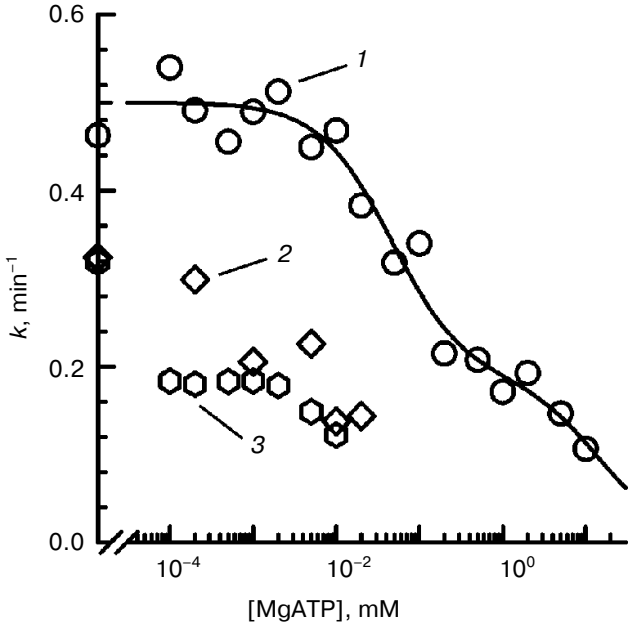

Fig. 3. Effect of MgATP concentration on the rate constant *k* of βY341W-$\alpha_3\beta_3\gamma$ subcomplex inhibition by 0.15 mM NBD-Cl in the absence (*1*) and presence of 0.06% LDAO (*2*) or 10 mM selenite (*3*). Rate constants *k* were obtained as described in "Materials and Methods". Line represents the best fit of the data obtained in the absence of LDAO and selenite (*1*) to Eq. (2), where K_{d2} and K_{d3} were substituted for $K_{½,2}$ and $K_{½,3}$, respectively, with the values of k_2, k_3, $K_{½,2}$, and $K_{½,3}$ equal to 0.31 ± 0.03 min^{-1}, 0.19 ± 0.03 min^{-1}, 46 ± 16 μM, and 15 ± 11 mM, respectively.

data were obtained in the presence of PEP and pyruvate kinase to prevent accumulation of MgADP during hydrolysis of ATP. Under these conditions, the rate constant *k* of βY341W-$\alpha_3\beta_3\gamma$ subcomplex inhibition by 0.15 mM NBD-Cl in the absence of nucleotide (0.46 min^{-1}) is about 30% smaller than the *k* value obtained in the absence of MgADP (0.68 min^{-1}; Fig. 2b). This difference is likely due to the presence of 1 mM PEP in the incubation medium during *k* measurements in the absence of MgATP. PEP was observed before to compete with MgATP for binding to catalytic sites of βY341W-$\alpha_3\beta_3\gamma$ subcomplex that contained additional αK175A/T176A-mutations affecting noncatalytic nucleotide-binding sites [58].

Fitting the data shown by circles in Fig. 3 to Eq. (2) where K_{d2} and K_{d3} were substituted for $K_{½,2}$ and $K_{½,3}$, respectively ($K_{½,2}$ and $K_{½,3}$ denote concentrations of MgATP required for half-maximal saturation of catalytic sites 2 and 3, respectively), resulted in the best fit values of k_2 and k_3 equal to 0.31 ± 0.03 and 0.19 ± 0.03 min^{-1}, respectively, and the best fit values of $K_{½,2}$ and $K_{½,3}$ equal to 46 ± 16 μM and 15 ± 11 mM, respectively. In this case also, indistinguishable results of the best fit were obtained when MgATP binding to catalytic sites 2 and 3 was assumed to be sequential. In the fluorescence quenching studies of βY341W-$\alpha_3\beta_3\gamma$ subcomplex, the catalytic site

with the lowest affinity was reported to exhibit a half-maximal saturation with MgATP at the nucleotide concentrations of 35 μM [24], 21 μM [32], 24 μM [33], 13 μM [25], and 38 μM [47]. All these values are significantly lower than the $K_{½,3}$ value of 15 mM obtained from the data shown in Fig. 3 (curve *1*), but correspond well to the $K_{½,2}$ value of 46 μM.

The data of Fig. 2b (curve *1*) and Fig. 3 (curve *1*) show that one of the catalytic sites of βY341W-$\alpha_3\beta_3\gamma$ subcomplex remains unoccupied at submillimolar concentrations of MgADP and MgATP and that this catalytic site has escaped detection by the fluorescence quenching method when the subcomplex was titrated by MgADP and MgATP. However, under the conditions used to obtain the data shown by curves *1* in Figs. 2b and 3 (a 2-mM excess of Mg^{2+} over the nucleotide), both the wild-type [59, 60] and βY341W-mutant [24, 49, 61] $\alpha_3\beta_3\gamma$ subcomplexes are known to form an inactive enzyme form. This inactive form is a result of MgADP (the so-called inhibitory MgADP) binding at one of the catalytic sites [62, 63]. Inhibitory MgADP renders the enzyme completely inactive [64, 65]. It has been shown first with MF_1 [66] and subsequently with the wild-type and βY341W-mutant $\alpha_3\beta_3\gamma$ subcomplexes [25, 56, 57, 67, 68] that formation of MgADP-inhibited form of the enzyme during ATP hydrolysis is responsible for deviations from the Michaelis–Menten behavior (see for example circles in Fig. 4). Therefore, to determine whether the low affinity of the catalytic site 3 to MgADP and MgATP observed in the experiments shown by curves *1* in Figs. 2b and 3, respectively, is an intrinsic characteristic of the active βY341W-$\alpha_3\beta_3\gamma$ subcomplex and is not due to MgADP-induced inhibition, the experiments were repeated in the presence of LDAO. LDAO is a well-known activator of TF_1 [69] and its wild-type [60] and βY341W-mutant [24, 31, 57, 61] (see also Fig. 4) $\alpha_3\beta_3\gamma$ subcomplexes and has been shown to act by releasing the MgADP-induced inhibition [59, 65].

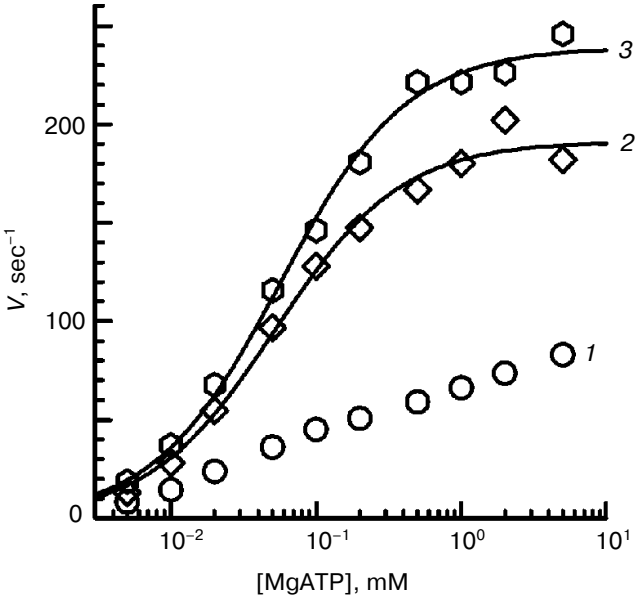

Fig. 4. Effect of MgATP concentration on the steady-state activity of βY341W-$\alpha_3\beta_3\gamma$ subcomplex in the absence (*1*) and presence of 0.06% LDAO (*2*) or 10 mM selenite (*3*) at room temperature. Lines represent the best fit of the data to the Michaelis–Menten equation with K_m and V_{max} values equal to 52 ± 5 μM and 191 ± 4 sec^{-1}, respectively, in the presence of LDAO (*2*), and 57 ± 4 μM and 239 ± 4 sec^{-1}, respectively, in the presence of selenite (*3*).

The effect of MgADP on the inhibition of βY341W-$\alpha_3\beta_3\gamma$ subcomplex by NBD-Cl in the presence of 0.06% LDAO is shown by diamonds in Fig. 2b (curve *2*). It is seen that, in the absence of MgADP, LDAO decreases the rate constant of inhibition k by about 25%. In the presence of LDAO, MgADP at concentrations up to 0.2 mM does not affect the inhibition of βY341W-$\alpha_3\beta_3\gamma$ subcomplex by NBD-Cl, but at the higher concentrations slows down the inhibition. Fitting these data to a hyperbolic equation:

$$k = k_0/(1 + S/K_d), \quad (3)$$

where k_0 is the rate constant of inhibition in the absence of MgADP, S is the concentration of MgADP, and K_d is the dissociation constant for a catalytic site where MgADP binding in the presence of LDAO provides a complete protection of βY341W-$\alpha_3\beta_3\gamma$ subcomplex from inhibition by NBD-Cl, resulted in the best fit values for k_0 and K_d of 0.508 ± 0.008 min^{-1} and 12 ± 2 mM, respectively (dashed curve *2* in Fig. 2b). The latter value (12 mM) is significantly higher than the K_d values for the lowest affinity catalytic site of 69 μM [24], 43 μM [32], and 50 μM [48] obtained for MgADP in the presence of LDAO using the fluorescence quenching method.

Diamonds in Fig. 3 show the effect of MgATP on the inhibition of βY341W-$\alpha_3\beta_3\gamma$ subcomplex by NBD-Cl in the presence of 0.06% LDAO. It is seen that, in the absence of nucleotide, LDAO decreases the rate constant of inhibition k by about 30%, and that increasing MgATP concentration to 20 μM results in an additional about 2-fold decrease of k. However, we were unable to obtain k values at the higher MgATP concentrations in the presence of LDAO, for under these conditions, in the absence of NBD-Cl, βY341W-$\alpha_3\beta_3\gamma$ subcomplex showed a decrease in activity of about 20% or more after prolonged incubations required for accurate measurements of low k values. Similar results shown by hexagons in Fig. 3 were obtained when we used 10 mM $KHSeO_3$ as an activator. Selenite is one of MF_1-activating anions [70]. It has been shown to activate EcF_1 [22] and is as effective as LDAO in activating βY341W-$\alpha_3\beta_3\gamma$ subcomplex of TF_1 (curve *3* in Fig. 4). Since the K_m values for MgATP in the presence of LDAO and selenite are equal to 52 and 57 μM, respectively (Fig. 4), the data obtained in the presence of activators and shown by diamonds and hexa-

gons in Fig. 3 are not sufficient to ascertain whether the active βY341W-$\alpha_3\beta_3\gamma$ subcomplex remains sensitive to inhibition by NBD-Cl at saturating MgATP concentrations and therefore has one catalytic site unoccupied, which would be indicative of a bi-site catalytic mechanism. To resolve this question, the extent of inhibition of βY341W-$\alpha_3\beta_3\gamma$ subcomplex by 0.15 mM NBD-Cl during MgATP hydrolysis in the presence of LDAO or selenite was measured after the enzyme incubation in the presence of the inhibitor for a short time, 2.5 min. Under these conditions, both in the absence and presence of MgATP, no decrease of the βY341W-$\alpha_3\beta_3\gamma$ subcomplex activity occurred in the absence of NBD-Cl. The results obtained in the presence of LDAO (diamonds) and selenite (hexagons) are shown in Fig. 5. It is seen that, in the presence of either activator, increasing MgATP concentration to 0.1-1 mM decreases the extent of the βY341W-$\alpha_3\beta_3\gamma$ subcomplex inhibition by NBD-Cl about 2-fold, but further increase of MgATP concentration results in no additional protection from the inhibition. Since the K_m for MgATP in the presence of LDAO and selenite is about 50 μM (Fig. 4), these results are inconsistent with a tri-site mechanism of ATP hydrolysis by the βY341W-$\alpha_3\beta_3\gamma$ subcomplex, but are in agreement with a bi-site mechanism of catalysis.

The result that activators LDAO and selenite in the absence of nucleotides partially protect βY341W-$\alpha_3\beta_3\gamma$ subcomplex from inhibition by NBD-Cl (Figs. 2b and 3) is similar to partial protection of the wild-type EcF_1 from inhibition by NBD-Cl exerted by selenite [44]. In the case of EcF_1, MgATP in the absence of selenite protected the enzyme from inhibition by NBD-Cl only partially, but a complete protection by MgATP was observed in the presence of selenite. On the basis of these observations it has been suggested that stimulation of ATP hydrolysis by activating anions is due to anion binding to the catalytic site that remains free of the nucleotide at saturating substrate concentration [44]. Partial protection of βY341W-$\alpha_3\beta_3\gamma$ subcomplex by LDAO and selenite in the absence of nucleotides (Figs. 2b and 3) suggests that in this enzyme activators also bind to a catalytic site. This suggestion is supported by the observation of Matsui et al. [65] that LDAO is able to activate a mutant $\alpha_3\beta_3\gamma$ subcomplex of TF_1 that lacks noncatalytic nucleotide-binding sites. However, lack of complete protection of βY341W-$\alpha_3\beta_3\gamma$ subcomplex from inhibition by NBD-Cl in the presence of MgATP and activators leaves a possibility open that in this enzyme the activators may bind outside of a catalytic site.

The results obtained show that βY341W-$\alpha_3\beta_3\gamma$ subcomplex remains susceptible to inhibition by NBD-Cl at MgADP and MgATP concentrations that has been shown to induce practically complete fluorescence quenching [24, 25, 32, 33, 47-49]. In the absence of an activator, a complete protection from NBD-Cl-induced inhibition by MgADP (curve *1* in Fig. 2b) and MgATP (curve *1* in Fig. 3) occurs with the nucleotide binding to a catalytic site with a K_d of 12 and 15 mM, respectively. In addition, in the presence of LDAO, MgADP protects βY341W-$\alpha_3\beta_3\gamma$ subcomplex from inhibition by NBD-Cl by binding to a catalytic site with a K_d of 12 mM (curve *2* in Fig. 2b). The fact that such catalytic-site binding of MgADP and MgATP has not been detected in the fluorescence quenching experiments [24, 25, 32, 33, 47-49] suggests that in βY341W-$\alpha_3\beta_3\gamma$ subcomplex of TF_1, as in βY331W-mutant EcF_1 [27, 44], nucleotide binding to the third (lowest affinity) catalytic site contributes little if at all to the total nucleotide-induced fluorescence quenching. Such a circumstance might have contributed to a mistaken interpretation of the fluorescence quenching results obtained with the βY341W-$\alpha_3\beta_3\gamma$ subcomplex of TF_1 [24, 25, 32, 33, 57] in a favor of a tri-site mechanism.

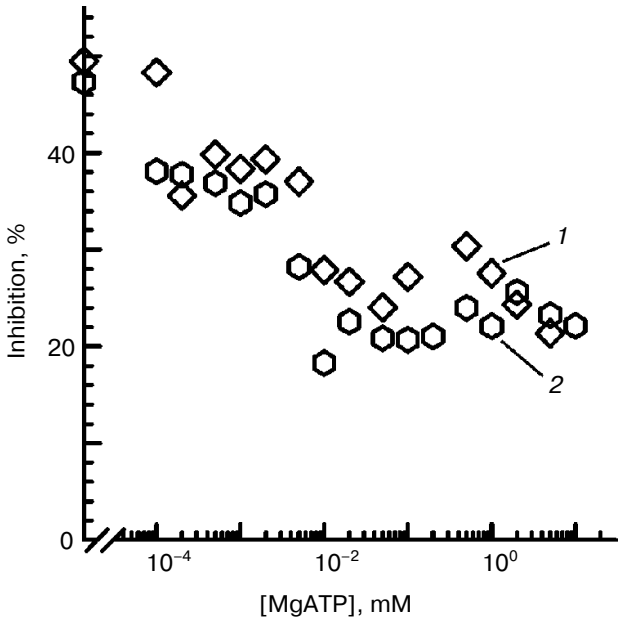

Fig. 5. Effect of substrate concentration on βY341W-$\alpha_3\beta_3\gamma$ subcomplex inhibition by NBD-Cl during MgATP hydrolysis in the presence of 0.06% LDAO (*1*) or 10 mM selenite (*2*). Ten nanomolar βY341W-$\alpha_3\beta_3\gamma$ subcomplex was preincubated at room temperature in MTE buffer containing additionally 10 mM CH_3COOK, 2.2 mM $Mg(CH_3COO)_2$, 1.5 mM PEP, 0.2 mg/ml pyruvate kinase, 0.3 mg/ml BSA, and either 0.06% LDAO (*1*) or 10 mM selenite (*2*) in the absence and presence of MgATP, then additionally incubated for 2.5 min in the presence of 0.15 mM NBD-Cl, and ATPase activity was measured as described in "Materials and Methods". Preincubation time in the presence of selenite was 8 min and in the presence of LDAO varied from 15 min at MgATP concentrations below 0.1 mM to 3 min at MgATP concentrations above 1 mM.

I thank Dr. Masasuke Yoshida and Dr. Toshiharu Suzuki for providing βY341W-$\alpha_3\beta_3\gamma$ subcomplex of TF_1, Dr. Richard L. Cross for support, and Dr. Paul D. Boyer for instigating this project and many discussions.

REFERENCES

1. Cross, R. L., and Nalin, C. M. (1982) *J. Biol. Chem.*, **257**, 2874-2881.
2. Kato-Yamada, Y., and Yoshida, M. (2003) *J. Biol. Chem.*, **278**, 36013-36016.
3. Iizuka, S., Kato, S., Yoshida, M., and Kato-Yamada, Y. (2006) *Biochem. Biophys. Res. Commun.*, **349**, 1368-1371.
4. Abrahams, J. P., Leslie, A. G., Lutter, R., and Walker, J. E. (1994) *Nature*, **370**, 621-628.
5. Boyer, P. D., Cross, R. L., and Momsen, W. (1973) *Proc. Natl. Acad. Sci. USA*, **70**, 2837-2839.
6. Kayalar, C., Rosing, J., and Boyer, P. D. (1977) *J. Biol. Chem.*, **252**, 2486-2491.
7. Boyer, P. D., and Kohlbrenner, W. E. (1981) in *Energy Coupling in Photosynthesis* (Selman, B. R., and Selman-Reiner S., eds.) Elsevier North Holland, New York, pp. 231-240.
8. Kinosita, K., Jr., Yasuda, R., Noji, H., and Adachi, K. (2000) *Philos. Trans. R. Soc. Lond. B, Biol. Sci.*, **355**, 473-489.
9. Stock, D., Gibbons, C., Arechaga, I., Leslie, A. G. W., and Walker, J. E. (2000) *Curr. Opin. Struct. Biol.*, **10**, 672-679.
10. Noji, H., Yasuda, R., Yoshida, M., and Kinosita, K., Jr. (1997) *Nature*, **386**, 299-302.
11. Kato-Yamada, Y., Noji, H., Yasuda, R., Kinosita, K., Jr., and Yoshida, M. (1998) *J. Biol. Chem.*, **273**, 19375-19377.
12. Sambongi, Y., Iko, Y., Tanabe, M., Omote, H., Iwamoto-Kihara, A., Ueda, I., Yanagida, T., Wada, Y., and Futai, M. (1999) *Science*, **286**, 1722-1724.
13. Nishio, K., Iwamoto-Kihara, A., Yamamoto, A., Wada, Y., and Futai, M. (2002) *Proc. Natl. Acad. Sci. USA*, **99**, 13448-13452.
14. Itoh, H., Takahashi, A., Adachi, K., Noji, H., Yasuda, R., Yoshida, M., and Kinosita, K., Jr. (2004) *Nature*, **427**, 465-468.
15. Cross, R. L., Grubmeyer, C., and Penefsky, H. S. (1982) *J. Biol. Chem.*, **257**, 12101-12105.
16. Grubmeyer, C., Cross, R. L., and Penefsky, H. S. (1982) *J. Biol. Chem.*, **257**, 12092-12100.
17. Cunningham, D., and Cross, R. L. (1988) *J. Biol. Chem.*, **263**, 18850-18856.
18. Zhou, J.-M., and Boyer, P. D. (1993) *J. Biol. Chem.*, **268**, 1531-1538.
19. Milgrom, Y. M., Murataliev, M. B., and Boyer, P. D. (1998) *Biochem. J.*, **330**, 1037-1043.
20. Murataliev, M. B., and Boyer, P. D. (1994) *J. Biol. Chem.*, **269**, 15431-15439.
21. Milgrom, Y. M., and Cross, R. L. (2005) *Proc. Natl. Acad. Sci. USA*, **102**, 13831-13836.
22. Bulygin, V. V., and Milgrom, Y. M. (2009) *Biochim. Biophys. Acta*, **1787**, 1016-1023.
23. Weber, J., Wilke-Mounts, S., Lee, R. S.-F., Grell, E., and Senior, A. E. (1993) *J. Biol. Chem.*, **268**, 20126-20133.
24. Dou, C., Fortes, P. A. G., and Allison, W. S. (1998) *Biochemistry*, **37**, 16757-16764.
25. Ono, S., Hara, K. Y., Hirao, J., Matsui, T., Noji, H., Yoshida, M., and Muneyuki, E. (2003) *Biochim. Biophys. Acta*, **1607**, 35-44.
26. Corvest, V., Sigalat, C., Venard, R., Falson, P., Mueller, D. M., and Haraux, F. (2005) *J. Biol. Chem.*, **280**, 9927-9936.
27. Bulygin, V. V., and Milgrom, Y. M. (2007) *Proc. Natl. Acad. Sci. USA*, **104**, 4327-4331.
28. Lobau, S., Weber, J., Wilke-Mounts, S., and Senior, A. E. (1997) *J. Biol. Chem.*, **272**, 3648-3656.
29. Weber, J., and Senior, A. E. (1998) *J. Biol. Chem.*, **273**, 33210-33215.
30. Nadanaciva, S., Weber, J., and Senior, A. E. (1999) *J. Biol. Chem.*, **274**, 7052-7058.
31. Weber, J., and Senior, A. E. (1995) *J. Biol. Chem.*, **270**, 12653-12658.
32. Ren, H., and Allison, W. S. (2000) *J. Biol. Chem.*, **275**, 10057-10063.
33. Bandyopadhyay, S., Valder, C. R., Huynh, H. G., Ren, H., and Allison, W. S. (2002) *Biochemistry*, **41**, 14421-14429.
34. Ahmad, Z., and Senior, A. E. (2004) *J. Biol. Chem.*, **279**, 31505-31513.
35. Ahmad, Z., and Senior, A. E. (2004) *J. Biol. Chem.*, **279**, 46057-46064.
36. Ahmad, Z., and Senior, A. E. (2005) *FEBS Lett.*, **579**, 523-528.
37. Nadanaciva, S., Weber, J., and Senior, A. E. (1999) *Biochemistry*, **38**, 7670-7677.
38. Nadanaciva, S., Weber, J., Wilke-Mounts, S., and Senior, A. E. (1999) *Biochemistry*, **38**, 15493-15499.
39. Ferguson, S. J., Lloyd, W. J., Lyons, M. H., and Radda, G. K. (1975) *Eur. J. Biochem.*, **54**, 117-126.
40. Andrews, W. W., Hill, F. C., and Allison, W. S. (1984) *J. Biol. Chem.*, **259**, 8219-8225.
41. Sutton, R., and Ferguson, S. J. (1985) *Eur. J. Biochem.*, **148**, 551-554.
42. Verburg, J. G., Yoshida, M., and Allison, W. S. (1986) *Arch. Biochem. Biophys.*, **245**, 8-13.
43. Yoshida, M., and Allison, W. S. (1990) *J. Biol. Chem.*, **265**, 2483-2487.
44. Bulygin, V. V., and Milgrom, Y. M. (2010) *Biochemistry (Moscow)*, **75**, 327-335.
45. Weber, J., Dunn, S. D., and Senior, A. E. (1999) *J. Biol. Chem.*, **274**, 19124-19128.
46. Mao, H. Z., Gray, W. D., and Weber, J. (2006) *FEBS Lett.*, **580**, 4131-4135.
47. Mnatsakanyan, N., Krishnakumar, A. M., Suzuki, T., and Weber, J. (2009) *J. Biol. Chem.*, **284**, 11336-11345.
48. Yasuno, T., Muneyuki, E., Yoshida, M., and Kato-Yamada, Y. (2009) *Biochem. Biophys. Res. Commun.*, **390**, 230-234.
49. Mitome, N., Ono, S., Suzuki, T., Shimabukuro, K., Muneyuki, E., and Yoshida, M. (2002) *Eur. J. Biochem.*, **269**, 53-60.
50. Suzuki, T., Murakami, T., Iino, R., Suzuki, J., Ono, S., Shirakihara, Y., and Yoshida, M. (2003) *J. Biol. Chem.*, **278**, 46840-46846.
51. Penefsky, H. S. (1977) *J. Biol. Chem.*, **252**, 2891-2899.
52. Noji, H., Bald, D., Yasuda, R., Itoh, H., Yoshida, M., and Kinosita, K., Jr. (2001) *J. Biol. Chem.*, **276**, 25480-25486.
53. Hossain, M. D., Furuike, S., Maki, Y., Adachi, K., Ali, M. Y., Huq, M., Itoh, H., Yoshida, M., and Kinosita, K., Jr. (2006) *Biophys. J.*, **90**, 4195-4203.
54. Shimabukuro, K., Yasuda, R., Muneyuki, E., Hara, K. Y., Kinosita, K., Jr., and Yoshida, M. (2003) *Proc. Natl. Acad. Sci. USA*, **100**, 14731-14736.
55. Pullman, M. E., Penefsky, H. S., Datta, A., and Racker, E. (1960) *J. Biol. Chem.*, **235**, 3322-3329.

56. Yasuda, R., Noji, H., Yosida, M., Kinosita, K., Jr., and Itoh, H. (2001) *Nature*, **410**, 898-904.
57. Ren, H., Bandyopadhyay, S., and Allison, W. S. (2006) *Biochemistry*, **45**, 6222-6230.
58. Shimo-Kon, R., Muneyuki, E., Sakai, H., Adachi, K., Yoshida, M., and Kinosita, K., Jr. (2010) *Biophys. J.*, **98**, 1227-1236.
59. Paik, S. R., Jault, J.-M., and Allison, W. S. (1994) *Biochemistry*, **33**, 126-133.
60. Jault, J.-M., Matsui, T., Jault, F. M., Kaibara, C., Muneyuki, E., Yoshida, M., Kagawa, Y., and Allison, W. S. (1995) *Biochemistry*, **34**, 16412-16418.
61. Dou, C., Grodsky, N. B., Matsui, T., Yoshida, M., and Allison, W. S. (1997) *Biochemistry*, **36**, 3719-3727.
62. Yoshida, M., and Allison, W. S. (1986) *J. Biol. Chem.*, **261**, 5714-5721.
63. Milgrom, Y. M., and Boyer, P. D. (1990) *Biochim. Biophys. Acta*, **1020**, 43-48.
64. Milgrom, Y. M., and Cross, R. L. (1993) *J. Biol. Chem.*, **268**, 23179-23185.
65. Matsui, T., Muneyuki, E., Honda, M., Allison, W. S., Dou, C., and Yoshida, M. (1997) *J. Biol. Chem.*, **272**, 8215-8221.
66. Vulfson, E. N., Drobinskaya, I. E., Kozlov, I. A., and Murataliev, M. B. (1986) *Biol. Membr. (Moscow)*, **3**, 339-351.
67. Jault, J.-M., Dou, C., Grodsky, N. B., Matsui, T., Yoshida, M., and Allison, W. S. (1996) *J. Biol. Chem.*, **271**, 28818-28824.
68. Sakaki, N., Shimo-kon, R., Adachi, K., Itoh, H., Furuiki, S., Muneyuki, E., Yoshida, M., and Kinosita, K., Jr. (2005) *Biophys, J.*, **88**, 2047-2056.
69. Paik, S. R., Yokoyama, K., Yoshida, M., Ohta, T., Kagawa, Y., and Allison, W. S. (1993) *J. Bioenerg. Biomembr.*, **25**, 679-684.
70. Ebel, R. E., and Lardy, H. A. (1975) *J. Biol. Chem.*, **250**, 191-196.